

Intact Size-Selected Au_n Clusters on a TiO₂(110)-(1 × 1) Surface at Room Temperature

Xiao Tong, Lauren Benz, Paul Kemper, Horia Metiu, Michael T. Bowers, and Steven K. Buratto*

Department of Chemistry and Biochemistry, University of California, Santa Barbara, California 93106

Received June 3, 2005; E-mail: buratto@chem.ucsb.edu

Nanoparticle size is an important parameter affecting the catalytic behavior of nanostructured metal/oxide catalysts.^{1–5} Heiz et al. showed that the catalytic activity of Au_n ($n \leq 20$) on MgO (100) films in the oxidation of CO was highest for Au₁₈ and that Au₈ was the smallest cluster which exhibited catalytic behavior.³ A similar investigation at room temperature involving Au_n ($n = 1–4, 7$) supported on rutile TiO₂(110) by Anderson et al. suggests a strong size dependence in the oxidation of CO, with significant reactivity for clusters as small as Au₃.⁴ While these two studies show a strong dependence of the catalytic activity on the deposited cluster size, the eventual size (and shape) of the metal clusters once they were deposited on the substrate was not measured directly in either case. It is well-known from scanning tunneling microscopy (STM) images of evaporated Au and Ag, assumed to be monomeric in the vapor phase, that these metals sinter upon reaching the surface of TiO₂ to form larger clusters ($\gg 10$ atoms).^{6–10} Additionally, the size distribution of clusters formed by depositing size-selected metal clusters on a substrate is often not well defined due to cluster diffusion and aggregation at low landing energies (a few eV/atom) or fragmentation and implantation at higher landing energies (~ 100 eV/atom), respectively.^{11,12} Thus, determining whether the mass-selected clusters deposited softly on a surface maintain their size after deposition is an important goal of research on catalysis by nanoclusters.¹³ In the experiments described here, we use ultrahigh vacuum (UHV) STM to image the shape and size of the Au_n⁺ clusters ($n = 1–8$) deposited with low kinetic energy on a single crystal rutile TiO₂(110)-(1 × 1) surface at room temperature. The atomic resolution STM images allow us to directly identify the shapes, adsorption sites, and size distributions of the adsorbed clusters.

The size-selected clusters of Au_n⁺ ($n = 1–8$) are created using laser desorption from a gold rod illuminated with a pulsed YAG laser beam (532 nm, 500 mJ/pulse max power), producing a gold plasma. Positive ion clusters are extracted and accelerated through a skimmer in an argon carrier gas. The clusters are then focused, further accelerated, and passed between the pole faces of a magnet, where the size-selection process occurs. The mass resolution is $\sim 10\%$. The size-selected cluster ion beam, which has a flux of ~ 1 nA/cm², is focused on a positively biased TiO₂(110)-(1 × 1) sample in a UHV chamber with a base pressure of less than 1×10^{-9} Torr during deposition. The sample bias is set to lower the incident kinetic energy of the clusters to less than 2.0 eV/atom, resulting in soft-landing conditions. Exposure times of 20–60 min at room temperature (RT) result in a surface coverage of $\sim 0.02–0.06$ ML for all the samples. Prior to cluster deposition, the clean TiO₂(110)-(1 × 1) surface was prepared by multiple cycles of Ar⁺ ion sputtering of the crystal (1 keV, 20 min), followed by flashing at ~ 850 °C. Empty state STM images of the surface were acquired at RT, in constant current mode, with a sample bias of +1 to +2 V and a tunneling current of 0.1–0.2 nA on an RHK SPM 100 in a chamber with base pressure of less than 2×10^{-10} Torr.

Figure 1A shows large clusters on the surface resulting from the deposition of Au₁⁺. A magnified region of this image, shown in Figure 1a, reveals that there are no small clusters on surface. These observations indicate that Au monomers are highly mobile on the rutile surface, leading to aggregation into larger clusters. Figure 2a shows a broad height distribution for the deposition of Au atoms with an average value of 4.3 Å (Figure 3) and a standard deviation of 1.7 Å. This result is similar to that observed from Au vapor deposition in the coverage region of 0.013–0.08 ML.¹⁸ These sintered clusters have an average lateral diameter of 14.8 ± 3.9 Å, which indicates that an average cluster contains on the order of tens of atoms.

Figure 1B shows an STM image taken after the deposition of Au₂⁺. In contrast to the monomer deposition, large, sintered clusters are rarely observed. Instead, a high density of very small clusters is seen, and most of them are located above the 5-fold coordinated titanium (5c-Ti) rows (Figure 1b). The height distribution is much narrower than that found in the case of the Au₁ deposition, as shown in Figure 2b. The clusters on the surface have an average height of 1.6 Å (Figure 3) and a standard deviation of 0.5 Å, suggesting that the adsorbed Au₂ clusters lay flat on the surface. The nearly uniform height and the preference for certain adsorption sites suggest that the adsorbed Au₂ clusters remain intact during landing.

Only small clusters are observed for Au₃⁺ (Figure 1C), and they are found mainly above the 5c-Ti rows (Figure 1c). The height distribution is narrow (Figure 2c) with an average value of 1.5 Å (Figure 3) and a standard deviation of 0.2 Å. As in the case of dimer deposition, this suggests that the adsorbed Au₃ are intact and that the clusters lay flat on the surface.

Small clusters were also observed after the deposition of Au₄⁺ (see Figure 1D and 1d). The height distribution for Au₄ clusters is shown in Figure 2d with an average height of 1.7 Å (Figure 3) and a standard deviation of 0.2 Å, suggesting that adsorbed Au₄ lays flat on the surface. The shape distribution of the Au₄ clusters on the surface is also interesting. The dominant shape is the two-lobe structure shown in Figure 1d. The center of the two lobes is always observed on a bridging O row. The average distance between the two lobes is about 7 Å (given the 5c-Ti row spacing of 6.5 Å, suggesting a quasi-linear structure, possibly with an elongated central Au–Au bond). The unique shape and sharp size distribution (Figure 2d) resulting from the deposition of Au₄ suggest the clusters remain intact on the surface.

Figure 1E shows small clusters resulting from the deposition of Au₅⁺. Most features are located over the 5c-Ti rows, as shown in Figure 1e. The height distribution is narrower than that of Au₁, but wider than that of Au₂, Au₃, and Au₄ (Figure 2e). The clusters have an average height of 2.6 ± 0.6 Å (Figure 3), suggesting that adsorbed Au₅, unlike Au₂, Au₃, and Au₄, is either strongly buckled or consists of two atomic layers.

Figure 1F and 1f shows features resulting from the deposition of Au₆⁺ clusters. Most features are located over the 5c-Ti rows.

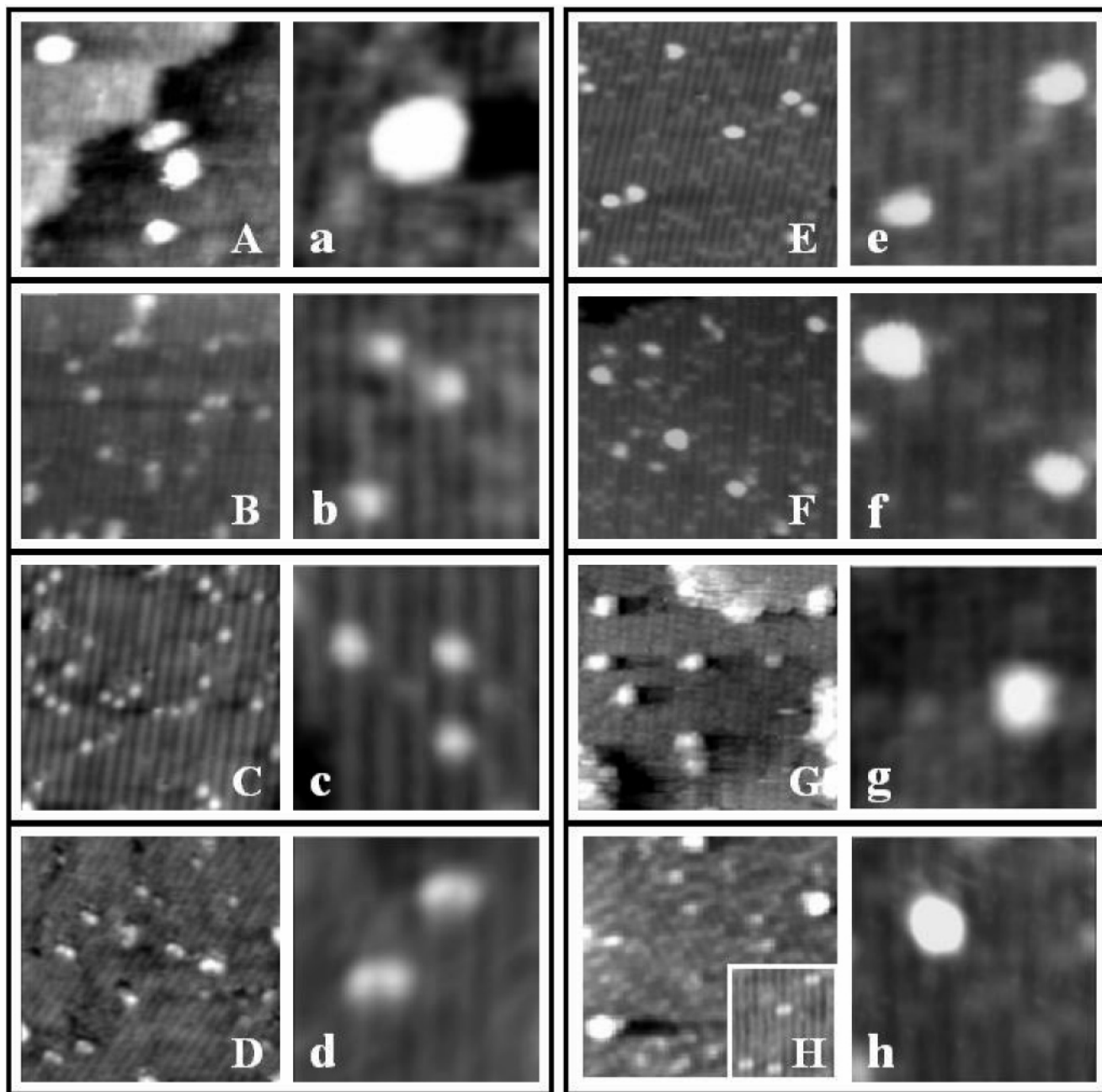


Figure 1. STM images $140 \text{ \AA} \times 140 \text{ \AA}$ (uppercase letters) and $50 \text{ \AA} \times 50 \text{ \AA}$ (lowercase letters) of the same surfaces, respectively. The bright spots are the clusters. The bright stripes are the 5-fold coordinated Ti atom (5c-Ti) rows separated by 6.5 \AA by the bridging oxygen rows, which are dark.¹⁴ The dim spots that appear on the bridging oxygen rows are bridging oxygen vacancies.^{10,15–17} (A/a) The TiO_2 surface after the deposition of Au_1 . (B/b) The same for Au_2 . (C/c) The same for Au_3 . (D/d) The same for Au_4 . (E/e) The same for Au_5 . (F/f) The same for Au_6 . (G/g) The same for Au_7 . (H/h) The same for Au_8 . The scale of the inset in H is $65 \text{ \AA} \times 75 \text{ \AA}$.

Their size distribution (Figure 2f) has an average height of $2.3 \pm 0.7 \text{ \AA}$ (Figure 3) and is similar to that of Au_5 , suggesting a buckled or a bilayer structure on the surface.

The result from the deposition of Au_7^+ is shown in Figure 1G and 1g. The height distribution (Figure 2g) shows an average height of $2.8 \pm 0.7 \text{ \AA}$ (Figure 3) for these clusters, which is similar to that obtained for both Au_5 and Au_6 . This suggests that the Au_7 clusters adopt a three-dimensional structure on surface. Most of the Au_7 clusters are located above the bridging oxygen rows (Figure 1g), which is different from both the Au_5 and Au_6 clusters. The unique adsorption site and slightly different height suggest the presence of intact Au_7 clusters on the surface.

Figures 1H and 1h show features resulting from deposition of Au_8^+ clusters. The height distribution (Figure 2h) gives an average

height of $2.7 \pm 0.9 \text{ \AA}$ (Figure 3) for these clusters. This suggests that the Au_8 clusters also adopt a three-dimensional structure on the surface with a similar average height as Au_5 , Au_6 , and Au_7 . The high-resolution STM image of Au_8 in the inset of Figure 1H shows that a small percentage (<5% of clusters) of the deposited Au_8 clusters dissociate to pairs of the two-lobed Au_4 species, which appear particularly stable on the $\text{TiO}_2(110)$ surface. No other cluster dissociations are observed for the systems reported here.

The results presented here are consistent with a number of earlier studies and provide some new, unexpected and important information. Soft-landing gold atoms lead to rapid sintering and formation of globules with an average height consistent with four atomic layers. Earlier STM studies on titania with larger coverages from evaporative gold sources indicated significant sintering and forma-

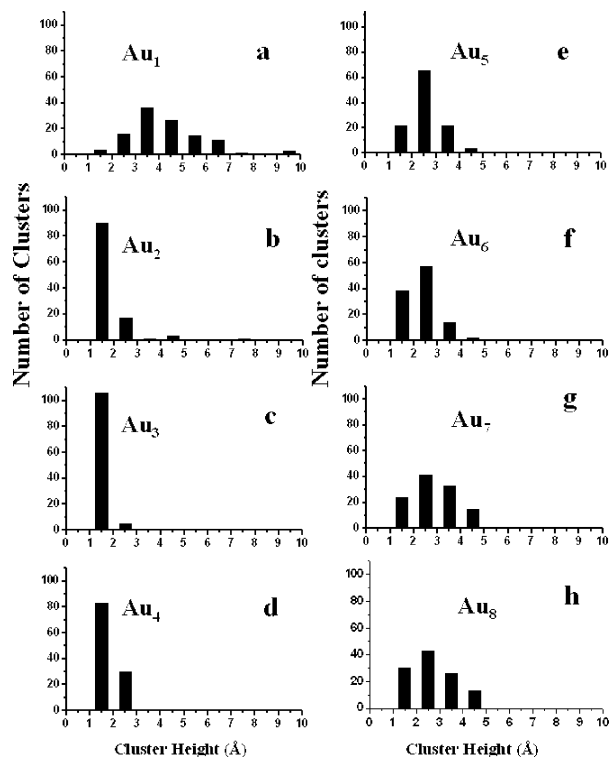


Figure 2. The cluster height distributions of deposited Au_n ($n = 1-8$) on $TiO_2(110)-(1 \times 1)$ surface.

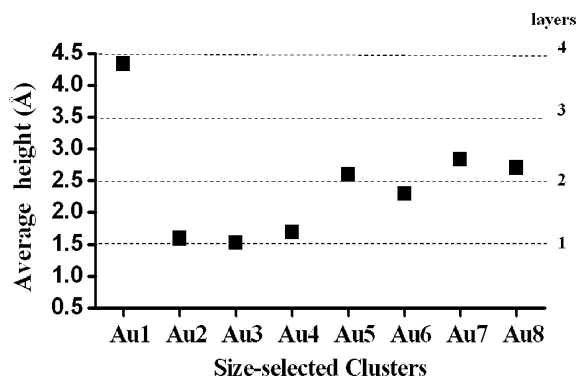


Figure 3. The average cluster heights of Au_n ($n = 1-8$) on the $TiO_2(110)-(1 \times 1)$ surface. The dashed lines indicate heights expected for various gold layers in the cluster.

tion of very large globules. Our low coverage, single atom depositions thus confirm the high mobility of Au atoms on titania and their tendency to sinter.

A surprise for us is the fact that clusters as small as the Au dimer have very limited mobility and do not sinter. By contrast, soft-landed silver dimers do sinter,¹⁹ forming globules of approximately the same size as the gold atom results presented here. Most likely, these results reflect the binding energies of silver and gold clusters to the surface of titania, which is a topic we will address in a future publication.

Gold dimers, trimers, and tetramers all lie flat on the surface, while Au_5 , Au_6 , Au_7 , and Au_8 all exhibit two-layer, three-dimensional structures. This is a surprising observation given that both theory and experiment indicate that isolated cationic gold clusters²⁰ are planar at least to Au_7^+ and that anionic gold clusters²¹ are planar to at least Au_{12}^- . The data in Figure 3 clearly indicate that the 2-d to 3-d transition occurs at $n = 5$ for neutral gold clusters on titania. Thus, the larger gold clusters bound to the surface adopt a different structure than in the gas phase.

The surface can have two effects on the gold cluster. First, electron transfer can occur from the surface to the cluster. This effect would favor planar structures based on gas-phase results.^{20,21} Second, the surface can specifically ligate the cluster. The primary ligation sites are the bridging oxygen atoms, separated by 6.5 Å between rows. The tetramer is the smallest cluster able to span across two adjacent rows and then only if a quasi-linear structure is invoked, a structure consistent with the two-lobed image we observe for Au_4 . This result suggests that surface ligation is driving cluster structure since the linear form of Au_4 is not favored by theory.²⁰ Recent results on both silver²² and gold²³ cluster cations indicate that gas-phase ligation can induce structural change consistent with this observation. The fact that the 2-d to 3-d transition occurs at Au_5 may reflect that the fifth gold atom is not needed for maximal ligation and begins to form a second layer in the cluster. The addition of the sixth and seventh gold atoms to the cluster continues the trend.

The importance of cluster–surface ligation is supported by the fact that the STM images observed were stable over several days and did not change with repeated scans by the STM tip. In addition, we observe a density of oxygen vacancies between clusters for all sizes studied here (see the high-resolution images in Figure 1a–1h). Generally, the density of oxygen vacancies is much higher than what would be expected if each cluster were bound to one or more oxygen vacancies. There is no direct evidence that these defects are required for binding the clusters. In fact, the lack of mobility of clusters as small as the dimer indicates that strong binding occurs with the stoichiometric surface.

Acknowledgment. This work was funded by a Defense University Research in Nanotechnology (DURINT) grant (F49620-01-04J9) from the Air Force Office of Scientific Research (AFOSR).

References

- (1) Haruta, M. *Catal. Today* **1997**, *36*, 153.
- (2) Valden, M.; Lai, X.; Goodman, D. W. *Science* **1998**, *281*, 1647.
- (3) Sanchez, A.; Abbet, S.; Heiz, U.; Schneider, W. D.; Hakkinen, H.; Barnett, R. N.; Landman, U. *J. Phys. Chem. A* **1999**, *103*, 9573.
- (4) Lee, S.; Fan, C.; Tainpin, W.; Anderson, S. L. *J. Am. Chem. Soc.* **2004**, *126*, 5682.
- (5) Yoon, B.; Hakkinen, H.; Landman, U.; Worz, A. S.; Antonietti, J. M.; Abbet, S.; Judai, K.; Heiz, U. *Science* **2005**, *307*, 403.
- (6) Lai, X.; St Clair, T. P.; Valden, M.; Goodman, D. W. *Prog. Surf. Sci.* **1998**, *59*, 25.
- (7) Lai, X. F.; Goodman, D. W. *J. Mol. Catal. A-Chem.* **2000**, *162*, 33.
- (8) Parker, S. C.; Grant, A. W.; Bondzie, V. A.; Campbell, C. T. *Surf. Sci.* **1999**, *441*, 10.
- (9) Wahlstrom, E.; Lopez, N.; Schaub, R.; Thosttrup, P.; Ronnau, A.; Africh, C.; Laegsgaard, E.; Norskov, J. K.; Besenbacher, F. *Phys. Rev. Lett.* **2003**, *90*, 026101.
- (10) Tong, X.; Benz, L.; Kolmakov, A.; Chretien, S.; Metiu, H.; Buratto, S. K. *Surf. Sci.* **2005**, *575*, 60.
- (11) Bromann, K.; Felix, C.; Brune, H.; Harbich, W.; Monot, R.; Buttet, J.; Kern, K. *Science* **1996**, *274*, 956.
- (12) Bromann, K.; Brune, H.; Felix, C.; Harbich, W.; Monot, R.; Buttet, J.; Kern, K. *Surf. Sci.* **1997**, *377*, 1051.
- (13) Schaub, R.; Jodicke, H.; Brunet, F.; Monot, R.; Buttet, J.; Harbich, W. *Phys. Rev. Lett.* **2001**, *86*, 3590.
- (14) Diebold, U. *Surf. Sci. Rep.* **2003**, *48*, 53.
- (15) Diebold, U.; Lehman, J.; Mahmoud, T.; Kuhn, M.; Leonardelli, G.; Hebenstreit, W.; Schmid, M.; Varga, P. *Surf. Sci.* **1998**, *411*, 137.
- (16) Suzuki, S.; Fukui, K.; Onishi, H.; Iwasawa, Y. *Phys. Rev. Lett.* **2000**, *84*, 2156.
- (17) Schaub, R.; Thosttrup, R.; Lopez, N.; Laegsgaard, E.; Stensgaard, I.; Norskov, J. K.; Besenbacher, F. *Phys. Rev. Lett.* **2001**, *87*, 6104.
- (18) Spiridis, N.; Haber, J.; Korecki, J. *Vacuum* **2001**, *63*, 99.
- (19) Benz, L.; Tong, X.; Kemper, P.; Lilach, Y.; Kolmakov, A.; Metiu, H.; Bowers, M. T.; Buratto, S. K. *J. Chem. Phys.* **2005**, *122*, 081102.
- (20) Gilb, S.; Weis, P.; Furche, F.; Ahlrichs, R.; Kappes, M. M. *J. Chem. Phys.* **2002**, *116*, 4094.
- (21) Furche, F.; Ahlrichs, R.; Weis, P.; Jacob, C.; Gilb, S.; Bierweiler, T.; Kappes, M. M. *J. Chem. Phys.* **2002**, *117*, 6982.
- (22) Manard, M.; Kemper, P.; Bowers, M. T. *J. Am. Chem. Soc.* **2005**, *127*, 9994.
- (23) Kemper, P.; Manard, M.; Bowers, M. T. Manuscript in preparation.

JA052778W